32nd Electric Vehicle Symposium (EVS32)
Lyon, France, May 19 - 22, 2019

Material Characterization and Analysis on the Effect of Vibration and Nail Penetration on Lithium ion Battery

P K Ajeet Babu[1], U S Karle[1], M R Saraf[1]

[1]*The Automotive Research Association of India, Pune, India*, ajeetbabu.fid@araiindia.com

Abstract

Battery packaging in a vehicle depends on the cell being used and its behavior plays an important role in the safety of the entire battery pack. Chemical degradation of various parts of cell such as cathode, anode is a concern as it adversely affects performance & safety. A cell in its battery pack once assembled can have two different mechanical abuse condition. One is the vibration generated from the vehicle and the second is the intrusion of external elements in case of accident. In this paper a commercially available 32700 lithium ion cell with LFP chemistry is studied for its response to both the abuse conditions at two different SoC. The primary aim of this study is to understand their effect on the surface morphology of the cathode and the anode. The cells are also characterized to study its impedance behavior before and after being abused mechanically. The cells tested for vibration were also analyzed for its dynamic stiffness. Microscopy techniques such as SEM images are used to study the surface morphology, EIS characterization is carried out to study the internal resistance of the cell. It is observed that there is a drop in internal resistance and increase in the stiffness after the cells subjected to mechanical abuse. The SEM study revealed different morphology at the center and at the corner for cell subjected to nail penetration at 50% SoC.

Keywords: Lithium Battery, Materials, Electrode, Internal Resistance, Safety.

1 Introduction

Lithium ion cells nowadays are used for various applications because of their great specific capacity, lower weight, and longer energy storage cycles. Today Li-ion cell has transformed from a device powering portable electronics to an energy solution for different sectors and automotive is one of the biggest beneficiary of this technology. This transformation has led to research for improving the energy density of LiB's [1-4]. A LiB contains electrolyte, separator, cathode and anode in different form factors such as cylindrical, prismatic and pouch. The cylindrical form factor varies from standard 18650 to new designs such as 21700, 32700 etc., Anode stores the Li^+ ions during charging and cathode acts as reservoir of Li^+ ions during discharging. There are various types of cathode materials developed in recent times to satisfy different functional requirements and also to store more energy. Olivine LiFePO4, which was first developed by Goodenough and his co-workers in 1997. It is the most promising cathode material for large-scale lithium ion batteries because of its safety and low cost [5-7]. Safety of cells is one of the primary requirement while being considered for any vehicular applications because the battery pack of any xEV consists of hundreds of cells connected in series or parallel to produce high voltage and current. The cell is subjected to vibration once mounted in the vehicle and the structural stability of the cell need to be evaluated for this condition. Various researchers have compared and stated that the vibration imparted in batteries is comparable with corresponding position of conventional cars [8-9]. USABC recommends both random vibration and sine harmonic vibration [10]. ECE R100.2 involves swept sine vibration only in the Z direction [11]. With respect to standards adopting sine vibrations, the acceleration suggested by USABC is much higher than the ECE standard. Apart from the

existing vibration which happens during the lifetime of the cell fitted in the vehicle, the cell may also experience extreme abuse such as in the event of an accident it is likely that an external object can get penetrated inside the battery pack. Penetration of cells by any sharp object can be one of the reasons for damage during such conditions. It is thus important to understand the behavior of the cell in these extreme abuse conditions too. The nail penetration test is recommended as per AIS 048[12]. A nail penetrated cell, along with a new cell, is generally used for further comparison by material characterization study.

Material characterization techniques by Scanning Electron Microscopy (SEM) with Energy Dispersive X-Ray Analysis (EDX) is one of the primary technique to study the morphology of the electrode and elemental composition. Changes taking place in the electrode of an abused cell is observed and can be compared with the electrodes of the new cell. In research work carried out by Wanga et al. SEM technique was used to study the cathode and anode of the 18650 Li-ion cell. According to their research, the SEM technique can be used to analyse the microscopic characteristic of surfaces and cross-sections of the electrodes. Schindler U. et al. used advanced SEM technology to study degradation phenomenon in Li-ion battery. They used detector strategies and voltage contrast to improve the resolution of SEM images of cell electrodes [13]. Liu et al. used EIS and SEM to check and relate the resistance stability of electrode and the morphology characteristics [14]. Morphology changes for Li/Li_3PS_4 and Li/Au/Li_3PS_4 were investigated using SEM analysis by A. Kato et al. SEM image analysis showed that the effect of gold (Au) thin film between Li metal and Li_3PS_4 electrolytes [15]. Babu P A et al. studied the performance of the cell by SEM analysis of Cathode and Anode for different abuse conditions [16]. The above researchers used SEM technique extensively for their study.

Electrochemical Impedance Spectroscopy (EIS) is another characterization technique that has revealed its importance and value through several applications [17]. It has been shown that it is a powerful device to characterize electrochemical processes occurring in a cell and to thereby estimate useful states indicators [18]. Therefore, it has become a major tool for investigating the properties of cells in EVs and HEVs [19-20]. Farhat et al. used EIS to study the charge transfer resistance and diffusion resistance of cell. Their research states that in EIS result, the charge transfer resistance is obtained at higher frequency range than the frequency of range of diffusion resistance [21]. Liu et al. in their work investigated the effect of microstructure morphology on the impedance response. They found out that the EIS curve varies with nature of reaction kinetics in the solid-electrolyte interface, exchange current density and dielectric property of the materials [22]. Illig et al. in this study, investigates the impedance response of an 18650 cell inside a frequency range of 100 kHz - 2 μHz by merging electrochemical impedance spectroscopy and time domain measurements. This study identified the dominating physical processes which were hidden in the impedance spectrum of the cell [23]. Though its robustness and high accuracy results, it is still more common in laboratory tests than in online field equipment.

Apart from material and electrochemical behavioural study, in recent times, various researchers have started to use mechanical behavior as an indicator of cell status [24-26]. Hooper et al claimed that the natural frequency of a Li-ion cells is independent on its SOC, but frequency information of the same cells with various SOCs was not investigated in his work [27]. Pham et al asserted a linear relationship between the SOC and frequency of a cell based on the fact that the FRF curves with different SOCs had similar spacing [28].

Various researchers have worked on characterizing the new cathode materials, but very few literature is available with respect to behavior of cell components with respect to external abuse conditions. In this research a commercially available LFP Chemistry based 32700 cylindrical form factor, LIB is selected for the study. The cell was subjected to two different abuse conditions i.e. Nail penetration and Sinusoidal vibration. Nail penetration was done at two different SoC i.e. 100% and 50% and vibration was carried out at 100% SoC. In case of nail penetration, the cells electrode morphology was studied using SEM technique along with EDS and in case of vibration the cells were characterized for its internal resistance and the dynamic stiffness. All the properties are compared with the benchmark condition of new cell.

2 Experimental setup

The batteries were charged under constant current and constant voltage protocol (CC-CV). Bitrod cell cycler is used for carrying out charging and discharging. The nail penetration test was carried out at two different SoC i.e. 100% and 50%. The cell is penetrated with a mild steel (conductive) pointed rod of 3 mm diameter, which was electrically insulated from the test fixture. The rate of penetration is kept at 8 cm/s. The orientation

of the penetration is perpendicular to the electrode plates. The cell is observed, with the rod remaining in place, for one hour after the test. The test is carried out using a hydraulic actuator.

Sinusoidal vibration test at single axis wherein the cell is vertically held was carried out in a single-axis shaker table. An aluminium fixture was designed in such a way that all degrees of freedom were arrested and the vibration effect is directly imparted to the internal structure of the cell. The top and bottom of the cell was covered with non-metal to prevent formation of any electrical connection. Refer Figure 1 for the experimental setup. Accelerometer were placed on the cells to measure the vibration profile and to control the tests. The test fixtures are properly secured to the shaker table and the frequency and G Value for the sinusoidal vibration in vertical direction is given in Table 1. Six numbers of cells were tested for both the abuse testing for statistical confidence.

Figure 1: Vibration test fixture and Setup

Table 1: Test Profile for Sinusoidal Vibration

Frequency Range(Hz)	Peak Acceleration (G)	Duration (min)
10-20	3.0	72
20-40	2.0	72
40-90	1.5	72
90-140	1.0	72
140-190	0.75	72

To carry out morphological analysis the samples were disassembled and the electrodes which were spirally wound together with the separator in between them were carefully taken out. The SEM was performed on samples electrodes of new and nail penetrated cell. The surface morphology study was done at different magnification and the voltage was kept as 20 KV. The compositional analysis is conducted using Energy Dispersive Spectroscopy (EDS) analyzer by Oxford detector. EIS is performed to check the internal resistance of the cell at a different SoC. EIS was done when the cell was fully charged in new cell and when it has completed vibration testing. The frequency range for EIS is kept high, and the minimum frequency is 10^{-2} Hz and the maximum frequency is 5 x 10^{5} Hz. The experimental setup which is used for calculation of dynamic stiffness is shown in Fig. 2. This setup consists of four batteries fixed in the vibration testing fixture, impact hammer, an accelerometer, analyzer (LMS). The fixture was rigidly fixed and the cell is mounted in vertical direction as in the real operating conditions. The hammer is used to excite the test specimen and the accelerometer is mounted on the top of the cell and used to record the input side acceleration. Calibration of sensors is done before each measurement. five averages are taken where the averages type is linear average. The resulting signals captured from the force transducer and accelerometer are then analysed by using LMS software. Refer Figure 2 for the experimental setup.

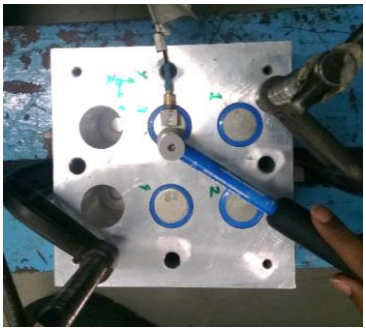

Figure 2: Dynamic Stiffness Measurement Set Up

3 Results and Discussion

3.1 Morphology Analysis

The surface morphology of the cathode and anode of the new cell is given in Figure 3 & 4 respectively. In case of samples which have undergone nail penetration at 50% SoC the location for composition analysis was done at two distinct places. The first location is at the centre of the cell where in the cylindrical rod has pierced the cell and the second location is at top of the electrode which is away from the centre where there is no physical damage during the testing. In case of samples which have undergone nail penetration at 50% SoC, in the anode there were no changes in morphology is observed when compared with new cells as shown in Figure 5, thus it can be stated that the material can be further used for recovery of carbon material. With respect to cathode, cracks were observed in the morphology of the grains as shown in Figure 6 and no other impurity or foreign elements presence were detected. The active material may be used again for reuse applications. In the centre location, the anode showed layer separation distinctly along with multiple cracks as shown in Figure 7. With respect to cathode the grains were completely destroyed and cracks were observed as shown in Figure 8.

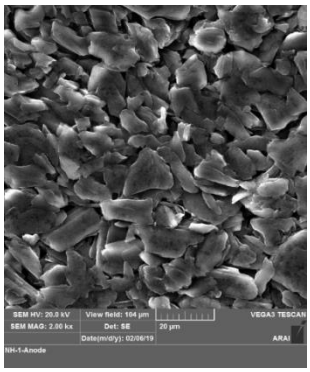

Figure 3: New Cell Anode

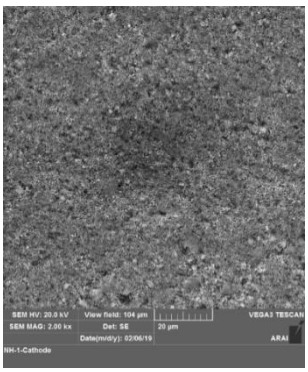

Figure 4: New Cell Cathode

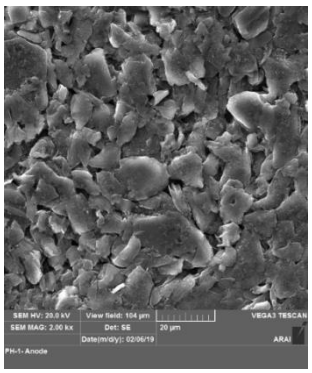

Figure 5: Nail Penetrated Cell Anode with location away from centre (50% SoC)

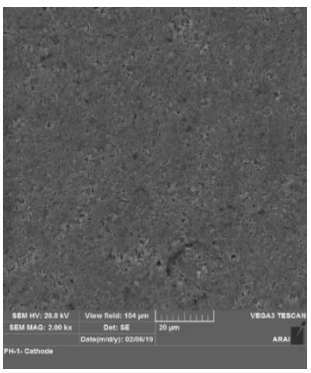

Figure 6: Nail Penetrated Cell Cathode with location away from centre (50% SoC)

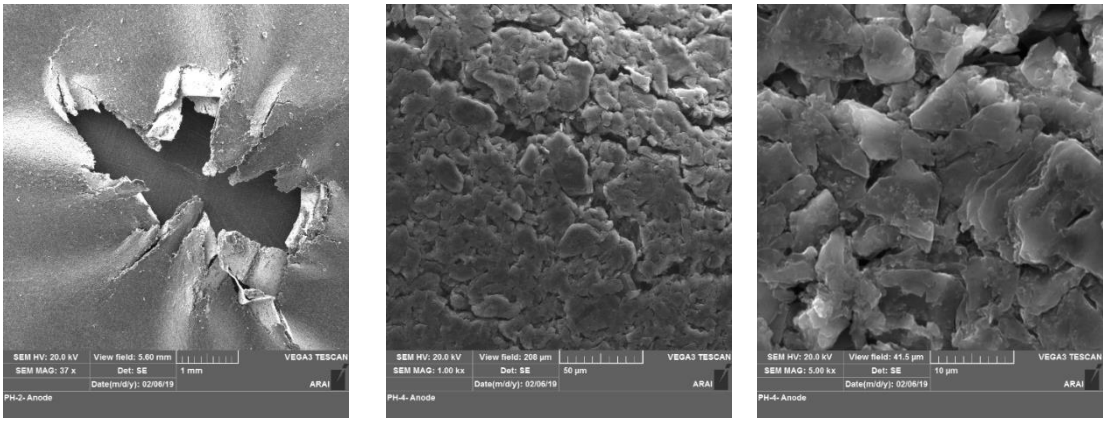

Figure 7: Nail Penetrated Cell Anode with location at centre (50% SoC)

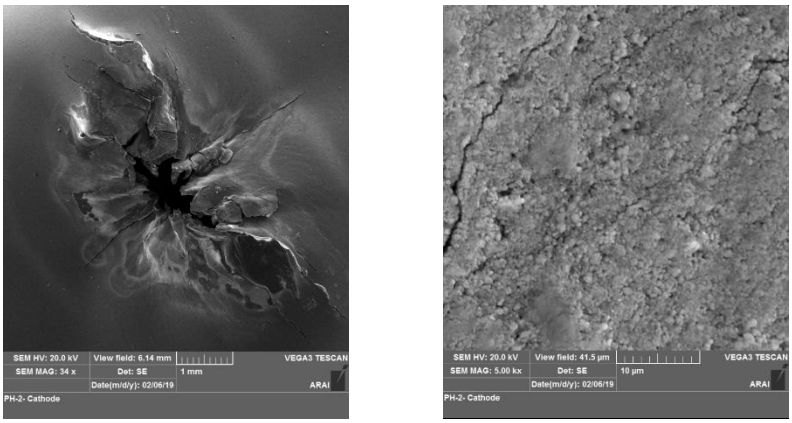

Figure 8: Nail Penetrated Cell Cathode with location at centre (50% SoC)

In case of samples which have undergone nail penetration at 100% SoC, the anode surface shows inhomogeneity in the grain structure and grain size was not uniform as shown in Figure 9. With respect to cathode carbon particles were observed which is due to transfer from anode and also structure was destroyed along with presence of solidification network as shown in Figure 10. In a new cell, the average grain size of the anode is 12 µm and 0.56 µm for the cathode. In case of nail penetrated samples the grain size of the anode reduced to 7 µm and grain size of cathode increased to 1 µm.

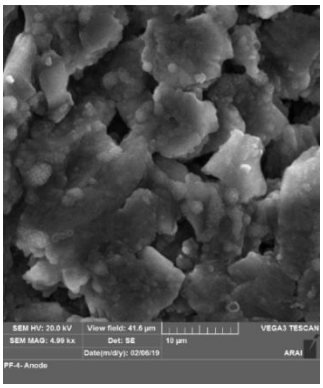

Figure 9: Nail Penetrated Cell Anode with location at centre (100% SoC)

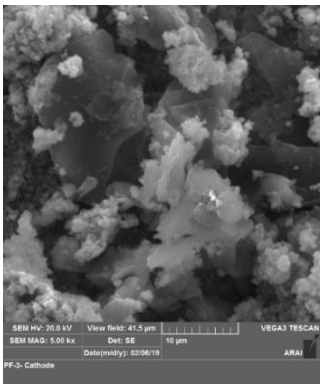

Figure 10: Nail Penetrated Cell Cathode with location at centre (100% SoC)

In case of samples which have undergone sinusoidal vibration at 100% SoC, the anode was found intact and was comparable with the surface of the new cell anode however, throughout the surface shows presence of tower like structure which has grown due to deposition of elements from the cathode as shown in Figure 11. This could have happened during the vibration testing of the cell. Similarly, in the cathode the structure was

fine with small spherical particles and agglomerates. The important observation is the formation of crater like structure on the active material as shown in Figure 12.

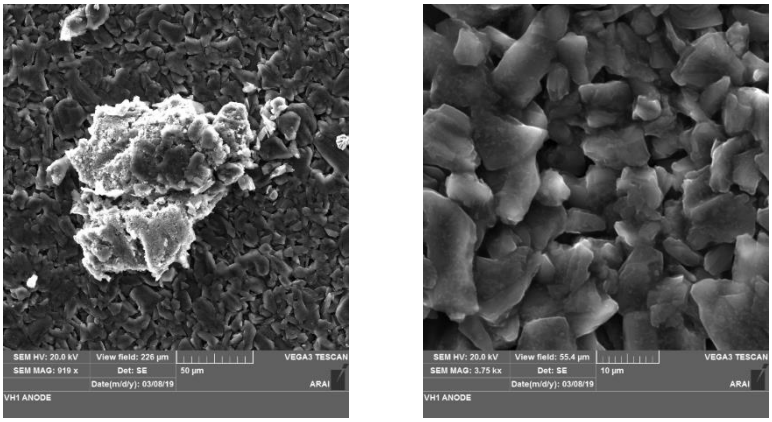

Figure 11: Anode of the cell after vibration testing

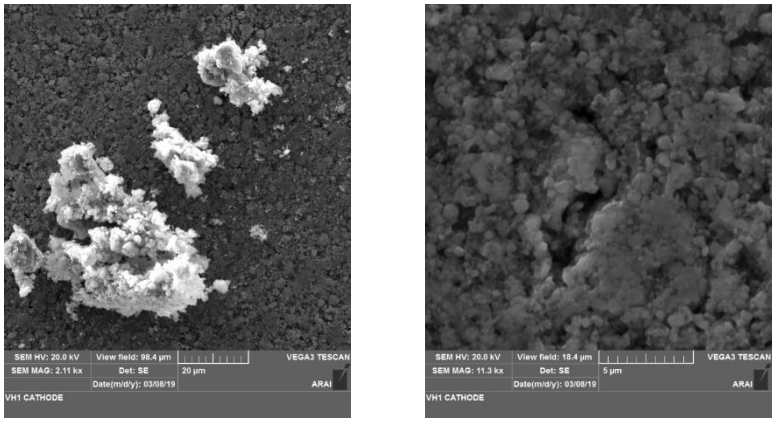

Figure 12: Anode of the cell after vibration testing

3.2 Composition Analysis

Electrodes of nail penetrated cell at 50% and 100% SoC and for the cell tested for vibration were measured for its elemental composition using EDS facility of the Scanning electron microscopy and further compared with the electrodes of the new cell. Totally six samples were tested and EDS readings are taken twice at each location for all samples.

In case of samples which have undergone nail penetration at 50% SoC the location for composition analysis was done at two distinct places as mentioned in the morphology study. With respect to cathode, In the second location the elemental Wt.% for C, O, P and Fe was similar for before and after testing and thus there is no effect of abuse on the distribution of the elements. In the centre, the amount of Iron increased from 26% to 52%, Phosphorus decreased from 16% to 8%, Oxygen decreased from 40% to 20% and Carbon decreased from 13% to 7.5%. It is thus can be said that when there is a localized mechanical damage to the cell without leading to complete destruction/explosion then that leads to uneven distribution of the elements within the cathode surface. With respect to anode, the elements such as C, O and P is found similar before and after the nail penetration test on the cell at both the locations.

In case of samples which have undergone nail penetration at 100% SoC, the cell was completely destroyed due to thermal runaway. With respect to cathode, the elemental distribution of cathode was similar to new cell. With respect to anode, the Carbon Wt.% dropped from 86% to 33% and Oxygen Wt.% increased from 6% to 48% and this could be due to the oxidation of the electrode due to thermal runaway. Traces of Iron element is observed in the destroyed anode.

In case of samples which have undergone sinusoidal vibration at 100% SoC, the cell was further disassembled and it is observed that the anode has additional deposition of Oxygen, Phosphorus and Iron which has come from the cathode, as compared to the new cell anode.

3.3 Internal Resistance Analysis

The cells were in 100% SoC capacity before the vibration test and the voltage is 3.3 V, after the test is over the voltage of each cell dropped by 0.3-0.4 V and this corresponds to 50% SoC capacity. The EIS Nyquist plot gives the behavior of the cell. The internal resistance of the new cell at 50% SoC is found to be 30-35 mΩ and the EIS of the cell after vibration test showed increase in the internal resistance by 5-25% as compared to the new cell. Six measurements were taken for each condition and the average value is reported. Refer Figure 13 & 14 for typical EIS Nyquist plot for new and abused cell (vibration tested). It is thus observed that there is increase in the internal resistance and performance of the cell has been hampered after the cell being subjected to vibration. One plausible explanation is of the fast increase of the resistance is that the surface film formed on the carbon electrode may not be as firm or protective as it is expected to be, especially during vibration. When there is a vibration load, the internal temperature is expected to increase. Ohm's law can easily explain this phenomenon. With more heat generated the internal pressure will also rise. The internal heat will not easily dissipate to the environment and the pressure will lead to gaseous release which will further lead to evaporation of electrolyte. This damages the surface film.

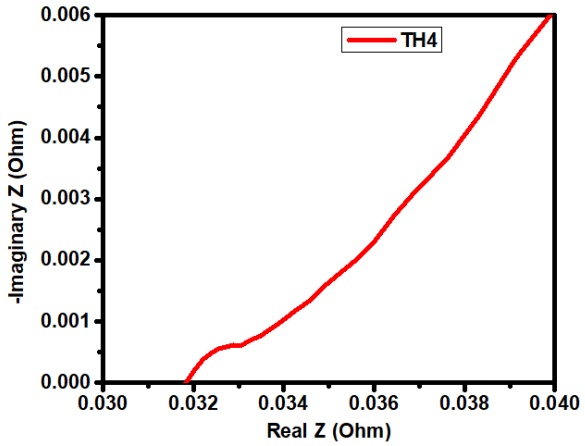

Figure 13: Nyquist Plot for New Cell

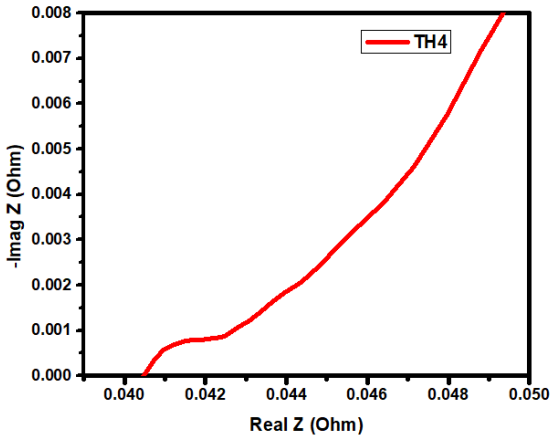

Figure 14: Nyquist Plot for Cell tested after Vibration testing

3.4 Dynamic Stiffness Analysis

The effect of vibration on the internal components of the LiB is one parameter studied as a part of the study. Frequency Response Function curve plot was drawn at two different state i.e. in the new cell and the post vibration testing. The maximum amplitude, frequency at maximum amplitude i.e. first mode resonance frequency and the corresponding dynamic stiffness of the cell was measured and given in Table 2 for cell without vibration and in Table 3 for cell with vibration.

It is thus observed that the average max amplitude was 14.6 $(m/s^2)/N$ and the corresponding frequency and dynamic stiffness was 172.5 Hz and 81.63 N/mm respectively. After the cell is tested for its vibration the average max amplitude increased to 16.7 $(m/s^2)/N$ i.e. 14% and the corresponding increase in the frequency and dynamic stiffness was 239.3 Hz and dynamic 138.83 N/mm i.e. 38% and 70% respectively. This increment in the dynamic stiffness could be attributed to the distributed mass of the cell components which was earlier acted as lumped mass before vibration. A typical FRF Curve for one cell is given in Figure 15 wherein shift in frequency and amplitude is clearly observed.

Table 2 : FRF Analysis of New Cell

Curve	Max amplitude (m/s^2)/N	Max amplitude's freq, Hz	Dynamic stiffness at Max amplitude freq (N/mm)
Cell 1	15.3	156.50	63.17
Cell 2	15.1	177.25	82.18
Cell 3	13.4	183.75	99.53
AVERAGE	**14.6**	**172.50**	**81.63**

Table 3 : FRF Analysis of Cell after Vibration

Curve	Max amplitude (m/s^2)/N	Max amplitude's freq, Hz	Dynamic stiffness at Max amplitude freq (N/mm)
Cell 1	17.0	216.5	109.09
Cell 2	15.3	270.5	188.45
Cell 3	17.7	231.0	118.96
AVERAGE	**16.7**	**239.3**	**138.83**

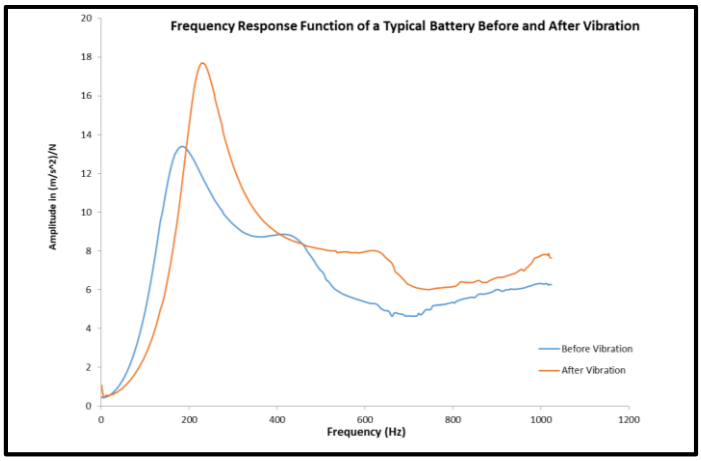

Figure 15: Typical FRF curve for cell before and after vibration

4 Conclusion

The cells were subjected to sinusoidal vibration and nail penetration at two different SoC. The following inference were drawn from the analysis: -

- Morphology analysis of vibration tested anode shows presence of tower like structure which has grown due to deposition of Fe and P elements from the cathode
- Compositional analysis shows that, when LiB undergoes a localized mechanical damage without thermal runaway then that leads to uneven distribution of the elements within the electrode surface
- In the top side location away from centre, for the cathode at 50% SoC nail penetrated samples, the elemental Wt.% for C, O, P and Fe was similar before and after testing and thus there is no effect of abuse on the distribution of the elements.

- Capacity fade happened in the cells which were in 100% SoC to 50% SoC as the voltage dropped by 0.3 to 0.4 V
- After the cell is tested for its sinusoidal vibration the average max amplitude, resonance frequency, dynamic stiffness and internal resistance increased by 14%, 38%, 70% and 25% respectively.
- FRF analysis of LiB can inform the state of cell and can be used as a non-destructive evaluation technique.
- It is important to validate the performance of LiB for its application and understanding the vibrational load during the lifetime of cell is to be carefully considered while designing the battery pack.

Acknowledgement

The authors would like to thank the team from Automotive Electronics Laboratory, Automotive Materials Laboratory and NVH laboratory of ARAI for their kind support on the characterization of the cells.

References

[1] Scrosati, B. and Garche, J., 2010. Lithium batteries: Status, prospects and future. Journal of power sources, 195(9), pp.2419-2430.

[2] Choi, N.S., Chen, Z., Freunberger, S.A., Ji, X., Sun, Y.K., Amine, K., Yushin, G., Nazar, L.F., Cho, J. and Bruce, P.G., 2012. Challenges facing lithium batteries and electrical double-layer capacitors. Angewandte Chemie International Edition, 51(40), pp.9994-10024.

[3] Owen, J.R. Rechargeable lithium batteries. Chem. Soc. Rev. 1997, 26, 259–267.

[4] Roberts, M., Johns, P., Owen, J., Brandell, D., Edstrom, K., El Enany, G., Guery, C., Golodnitsky, D., Lacey, M., Lecoeur, C. and Mazor, H., 2011. 3D lithium ion batteries—from fundamentals to fabrication. Journal of Materials Chemistry, 21(27), pp.9876-9890.

[5] Padhi, A.K., Nanjundaswamy, K.S. and Goodenough, J.B., 1997. Phospho-olivines as positive-electrode materials for rechargeable lithium batteries. Journal of the electrochemical society, 144(4), pp.1188-1194.

[6] Liu, H., Cao, Q., Fu, L.J., Li, C., Wu, Y.P. and Wu, H.Q., 2006. Doping effects of zinc on LiFePO4 cathode material for lithium ion batteries. Electrochemistry Communications, 8(10), pp.1553-1557.

[7] Chung, S.Y., Bloking, J.T. and Chiang, Y.M., 2002. Electronically conductive phospho-olivines as lithium storage electrodes. Nature materials, 1(2), p.123.

[8] Lang, J.F. and Kjell, G., 2015. Comparing vibration measurements in an electric vehicle with standard vibration requirements for Li-ion batteries using power spectral density analysis. International Journal of Electric and Hybrid Vehicles, 7(3), pp.272-286.

[9] Hooper, J.M. and Marco, J., 2014. Characterising the in-vehicle vibration inputs to the high voltage battery of an electric vehicle. Journal of power sources, 245, pp.510-519.

[10] Unkelhaeuser, T. and Smallwood, D., 1999. United States Advanced Battery Consortium Electrochemical Storage System Abuse Test Procedure Manual, USABC, USABC/SNL CRADA No. SC961447.

[11] ECE R100, Uniform provisions concerning the approval of vehicles with regard to specific requirements for the electric power train, 2013

[12] Automotive Industry Standard 048 - 2009 - Battery Operated Vehicles - Safety Requirements of Traction Batteries, India

[13] Golla-Schindler, U., Zeibig, D., Prickler, L., Behn, S., Bernthaler, T. and Schneider, G., 2018. Characterization of degeneration phenomena in lithium-ion batteries by combined microscopic techniques. Micron, 113, pp.10-19.

[14] Liu, S., Hong, X., Wang, D., Li, Y., Xu, J., Zheng, C. and Xie, K., 2018. Hollow carbon spheres with nanoporous shells and tailored chemical interfaces as sulfur host for long cycle life of lithium sulfur batteries. Electrochimica Acta, 279, pp.10-18.

[15] Kato, A., Kowada, H., Deguchi, M., Hotehama, C., Hayashi, A. and Tatsumisago, M., 2018. XPS and SEM analysis between Li/Li 3 PS 4 interface with Au thin film for all-solid-state lithium batteries. Solid State Ionics, 322, pp.1-4.

[16] Babu, P.A., Waghmare, A.S., Mulla, S.M., Karle, U.S. and Saraf, M.R., 2017, December. Material characterization of Lithium-ion battery cells by scanning electron microscopy & X-ray diffraction techniques. In 2017 IEEE Transportation Electrification Conference (ITEC-India) (pp. 1-5). IEEE.

[17] Barsoukov, E. and Macdonald, J.R. eds., 2018. Impedance spectroscopy: theory, experiment, and applications. John Wiley & Sons.

[18] Huet, F., 1998. A review of impedance measurements for determination of the state-of-charge or state-of-health of secondary batteries. Journal of power sources, 70(1), pp.59-69.

[19] Buller, S., 2002. Impedance based simulation models for energy storage devices in advanced automotive power systems. Shaker.

[20] Orazem, M.E. and Tribollet, B., 2011. Electrochemical impedance spectroscopy (Vol. 48). John Wiley & Sons.

[21] Farhat, D., Maibach, J., Eriksson, H., Edström, K., Lemordant, D. and Ghamouss, F., 2018. Towards high-voltage Li-ion batteries: Reversible cycling of graphite anodes and Li-ion batteries in adiponitrile-based electrolytes. Electrochimica Acta, 281, pp.299-311.

[22] Liu, S., Hong, X., Wang, D., Li, Y., Xu, J., Zheng, C. and Xie, K., 2018. Hollow carbon spheres with nanoporous shells and tailored chemical interfaces as sulfur host for long cycle life of lithium sulfur batteries. Electrochimica Acta, 279, pp.10-18.

[23] Illig, J., Schmidt, J.P., Weiss, M., Weber, A. and Ivers-Tiffée, E., 2013. Understanding the impedance spectrum of 18650 LiFePO4-cells. Journal of Power Sources, 239, pp.670-679.

[24] Samad, N.A., Kim, Y., Siegel, J.B. and Stefanopoulou, A.G., 2016. Battery capacity fading estimation using a force-based incremental capacity analysis. Journal of The Electrochemical Society, 163(8), pp. A1584-A1594.

[25] Dai, H., Yu, C., Wei, X. and Sun, Z., 2017. State of charge estimation for lithium-ion pouch batteries based on stress measurement. Energy, 129, pp.16-27.

[26] Cannarella, J. and Arnold, C.B., 2014. State of health and charge measurements in lithium-ion batteries using mechanical stress. Journal of Power Sources, 269, pp.7-14.

[27] Hooper, J.M. and Marco, J., 2015. Experimental modal analysis of lithium-ion pouch cells. Journal of Power Sources, 285, pp.247-259.

[28] Pham, H.L., Dietz, J.E., Adams, D.E. and Sharp, N.D., 2013, November. Lithium-ion battery cell health monitoring using vibration diagnostic test. In ASME 2013 International Mechanical Engineering Congress and Exposition (pp. V04BT04A048-V04BT04A048). American Society of Mechanical Engineers.

Authors

Dr P K Ajeet Babu has completed his doctorate in the area of aluminium deformation and has more than ten years of experience in process-structure-property-performance correlation studies. At Technology Group of ARAI, He is currently focussed on battery engineering with respect to carrying out destructive and non-destructive material characterization experiments to assess the state of battery for various battery chemistry. He is also working on developing methodology for Reduce, Reuse and Recycling of batteries. He is working with various leading research and academic institutes worldwide and providing services in the field of materials technology.